Journal of Alloys and Compounds 766 (2018) 640–648

Contents lists available at ScienceDirect

Journal of Alloys and Compounds

journal homepage: http://www.elsevier.com/locate/jalcom

Prediction of stable Cu-Li binary intermetallics from first-principles calculations: Stoichiometries, crystal structures, and physical properties

Jiahui Yu [b], Dawei Zhou [a, *], Chunying Pu [a, **], Xin Tang [c], Feiwu Zhang [d, e]

[a] College of Physics and Electronic Engineering, Nanyang Normal University, Nanyang 473061, China
[b] School of Electronic and Electrical Engineering, Nanyang Institute of Technology, Nanyang 473004, China
[c] College of Material Science and Engineering, Guilin University of Technology, Guilin 541004, China
[d] State Key Laboratory of Ore Deposit Geochemistry, Institute of Geochemistry, Chinese Academy of Sciences, Guiyang 550081, China
[e] School of Mathematics and Physics, Suzhou University of Science and Technology, Suzhou Jiangsu, 215009, China

ARTICLE INFO

Article history:
Received 27 March 2018
Received in revised form
27 June 2018
Accepted 2 July 2018
Available online 3 July 2018

Keywords:
Phase diagram
Intermetallics
First principle
Thermodynamic properties

ABSTRACT

Towards a resolution of the longstanding controversy regarding the existence of Cu-Li intermetallic compounds, we extensively investigate the phase stability of Cu-Li intermetallics with various possible stoichiometries at zero temperature and pressure using a global structure searching method. It is found that Cu-Li intermetallics can exist stably at atmospheric pressure, and three stable phases (*Fmmm* Cu_1Li_2, *Fd*$\bar{3}$*m* Cu_2Li_1, and *P*$\bar{1}$ Cu_7Li_1) are identified. Electronic structure analysis reveals that although they are metallic, covalent Cu-Cu and ionic Cu-Li bonds are found in the three structures. Moreover, the 3d states of copper atoms are mostly responsible for bond formations in the stable phases predicted. For all the predicted Cu-Li intermetallics, the effect of Cu concentration on structure, mechanical and thermodynamic properties are calculated systematically. It is found that the copper atoms in Cu-Li intermetallics trend to form covalent bonds, so more covalent bonds are formed as Cu content increases, leading to the increases in the elastic moduli, Vicker hardness and Debye temperature with Cu content on the whole. The Poisson's ratios of Cu-Li intermetallics vary in the range of 0.25 and 0.35, and most of Cu-Li intermetallics exhibit an excellent ductile property. The elastic anisotropy calculations suggest that all the Cu-Li intermetallics show anisotropic elasticity more or less, and the percentage anisotropy in compressibility is smaller than that in shear for each of the predicted Cu-Li compounds.

1. Introduction

Copper is an abundant, reasonably inexpensive transition metal. Copper and its alloys have been widely used in electric industry because of their excellent electrical conductivity. However, the impurities in Cu usually cause a decrease in electrical conductivity. It has been revealed that lithium can not only refine the impurities in copper but also increases the tensile strength of copper without the electrical conductivity decreasing [1]. However, there remains a great deal of controversy regarding the existence of Cu-Li intermediate phases over past eighty years. Both Pastorello [2] in 1930 and Klemm et al. [3] in 1958 showed that there are no intermediate phases in the Cu-Li phase diagram through X-ray analysis. Pelton [4] also believed that there are no intermediate phases in binary Cu-Li alloys based on the thermodynamic calculations. Saunders [5] further supported the nonexistence of Cu-Li intermetallic phases in 1998. On the contrary, Old and Treven [6] proposed a cubic Cu_4Li intermediate phase based on XRD investigations as early as 1981. Later, Penaloza et al. [7] and Borgstedt [8] accepted the existence of Cu_4Li. Van de Walle et al. [9] also suggested that Cu_4Li phase could exist probably based on *ab-initio* calculations. Besides Cu_4Li, Gąsior et al. [10] in 2009 proposed an intermetallic phase Cu_2Li_3 through electromotive force measurements, but they did not provide clear evidence. Okamoto [11] further accepted the existence of Cu_2Li_3 reported by Gąsior et al. [10]. Very recently, Li et al. [12] pointed out that the lattice parameters of the Cu_4Li phase proposed by Old and Treven et al. [6] fit well with the lattice parameters of fcc Cu. Therefore, Cu_4Li phase was considered to be part of fcc Cu, they also

* Corresponding author.
** Corresponding author.
E-mail addresses: zhoudawei@nynu.edu.cn (D. Zhou), puchunying@126.com (C. Pu).

https://doi.org/10.1016/j.jallcom.2018.07.020
0925-8388/

declared that they could not confirm the presence of Cu_2Li_3 using the powder XRD measurements. We noticed that the previous work [13,14] has shown that Au and Li can form stable intermetallic phases. It is also known that elements in the same group often have similar physical and chemical properties. Therefore, it seems possible for Cu and Li to form stable intermetallic phases in theory.

As is well known, first-principle calculations are based on the laws of quantum mechanics, which have been successfully applied to the investigations on the physical properties of binary and ternary alloys, such as phase diagram, electron structure, phonon curves, mechanical and thermodynamic properties [15–18]. So in this paper, we systematically explored the ground–state phases of Cu–Li system using evolutionary structure prediction algorithm USPEX and first principle calculations. We found that the stable Cu-Li intermetallics can be formed under normal conditions, and three stable Cu–Li intermetallic compounds, *Fmmm* Cu_1Li_2, $Fd\bar{3}m$ Cu_2Li_1 and $P\bar{1}$ Cu_7Li_1, were found. We further investigated systematically the physical properties of all the predicted ordered Cu-Li alloys as a function of Cu concentration, including the structure stability, formation enthalpy, phonon spectrum, electronic, mechanical and thermodynamic properties.

2. Theoretical method

In this work, structure searches for the stable Cu-Li intermetallic phases have been performed across the entire concentration range using the evolutionary algorithm-based method Universal Structure Predictor: Evolutionary Xtalloraphy (USPEX) [19,20], which has been successfully applied to predict structures of many systems from elemental solids to ternary compounds [21–27]. The structure searches were carried out up to 20 atoms in the unit cell for all possible stoichiometries. In each search, the first generation of structures was produced randomly and subsequently optimized. Each generation contains 30 structures. For the next generation, 60% of the structures were generated from the lowest-enthalpy structures provided by the previous generation, while 40% would be generated randomly. We usually followed 20 generations to achieve convergence of the sampling of the low-energy minima in configurational space. All the structural relaxations were performed within the framework of density functional theory using the Vienna *ab initio* Simulation Package [28,29] with the projector augmented wave (PAW) method [30]. The first-principles pseudopotential Perdew-Burke-Ernzerhof (PBE) approach was chosen as the exchange and correlation functional [31]. The PAW potentials treated $3d^{10}4s^1$ and $2s^1$ as the valence electrons for the Cu and Li, respectively. For structure prediction, a plane-wave kinetic energy cutoff of 360 eV and a k-point grid spacing of $2\pi \times 0.06$ Å^{-1} were used. When we calculated the enthalpy curves and electronic structures, a higher level of accuracy consisting of a basis set cutoff of 600 eV and a k-point grid spacing of $2\pi \times 0.03$ Å^{-1} was used, which ensured that those calculations were well-converged. During the structural optimization, all atoms were fully relaxed until the total energy changes and force less than 1.0×10^{-6} eV/atom, 0.002 eV/Å, respectively. Through the CASTEP code [32], the Mulliken overlap population was carried out using the pseudopotential plane wave technique, and the ultrasoft pseudopotential [33] was carried out with $3d^{10}4s^1$ and $1s^22s^1$ electrons as valence electrons for Cu and Li atoms, respectively. The phonon dispersion calculations were performed by using a supercell approach as implemented in the PHONOPY code [34,35]. The phonon calculations for Cu_1Li_2, $Cu_2Li_1$and Cu_7Li_1 were performed by using $1 \times 1 \times 2$, $2 \times 2 \times 2$ and $2 \times 2 \times 2$ supercells, respectively. The crystal structures of three stable structures are obtained as implemented in VESTA [36].

3. Results and discussion

3.1. Crystal structure and thermodynamic stability

Our structure searches successfully reproduced the experimentally observed fcc Cu and bcc Li at zero pressure, and the calculated lattice parameters agree well with experimental results [37] as shown in Table S1. In order to describe the thermodynamical stability of Cu-Li alloys, we calculated their formation enthalpies. The enthalpy of formation ΔH can be calculated from the following relation:

$$\Delta H = [E(Cu_mLi_n) - mE(\text{Solid Cu}) - nE(\text{Solid Li})]/(m+n) \quad (1)$$

where Δ*H* is defined as the relative formation enthalpy per atom of a compound of this stoichiometry, and $E(Cu_mLi_n)$ is the total energy/formula unit of the compound, E(Solid Cu) and E(Solid Li) are the total energies of the pure elements in their most stable state, and *m* and *n* are the number of Cu and Li atoms for a system, respectively. In general, a negative formation enthalpy means that the crystal can exist stably. Moreover, the more negative formation enthalpy indicates, the higher stability of crystal. In Fig. 1, the convex hull connects the phases with the lowest formation enthalpies among all compositions, and any phases lying exactly on the convex hull are deemed as energetically stable. The structures whose enthalpies remain above the convex hull would be thermodynamically metastable. From Fig. 1, we can conclude that stable intermetallic phases of Cu-Li alloys can be formed at zero pressure due to a negative enthalpy of formation from Cu and Li. For the considered Cu-Li compounds, three stable structures are found, i.e., Cu_1Li_2, Cu_2Li_1 and Cu_7Li_1. The schematic illustrations of them are shown in Fig. 2. The corresponding lattice parameters and atomic positions are listed in Table S2. Cu_1Li_2 crystalizes in an orthorhombic structure with space group *Fmmm*. From a structural point of view, *Fmmm* Cu_1Li_2 can be regarded as a layered structure. In this structure, an isosceles triangle unit consisted of three Cu atoms is found, and many such units form a coplanar Cu layer, while Li atoms form two puckered layers between the two Cu-layers. The Cu-Cu bond distances in Cu_1Li_2 are 2.475 and 2.505 Å, respectively, which are shorter than those in fcc Cu (2.556 Å), so there may exist a stronger interrelation among the Cu atoms in Cu_1Li_2. The most stable stoichiometry is Cu_2Li_1, which has a cubic structure with

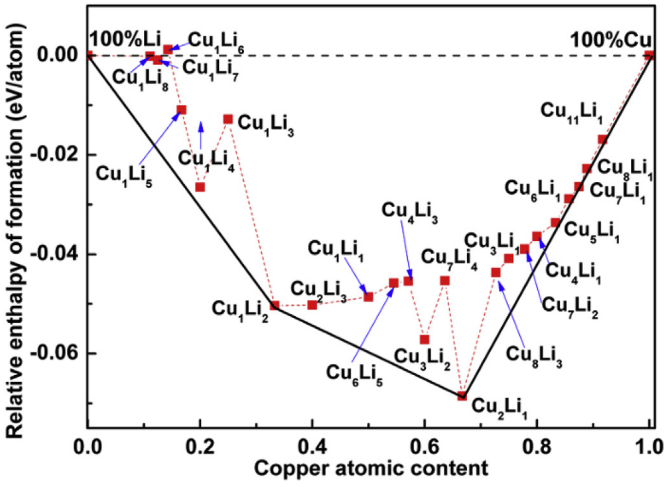

Fig. 1. The convex hull of the Cu–Li system at atmospheric pressure. The black line indicates the ground-state convex hull. The fcc-Cu and bcc-Li are used as the reference states.

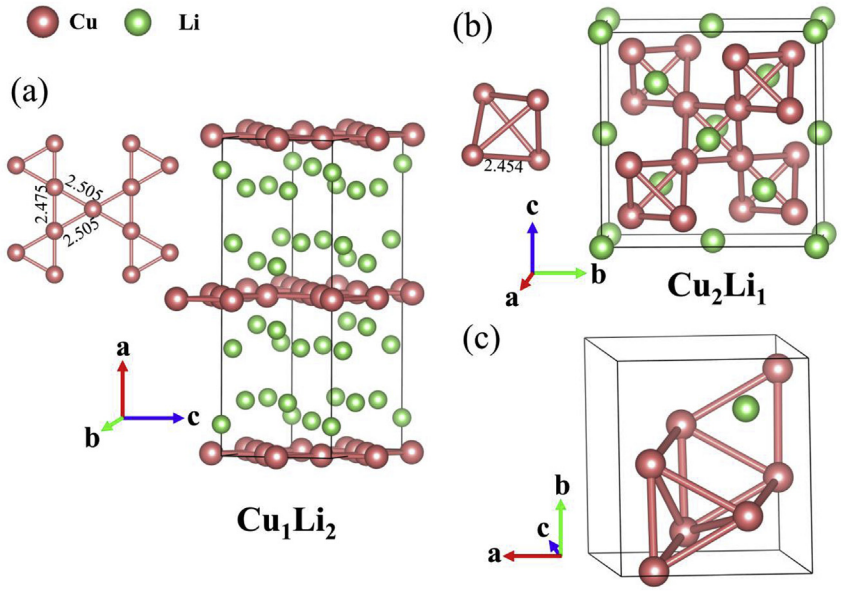

Fig. 2. The unit cells of (a) Cu_1Li_2, (b) Cu_2Li_1 and (c) Cu_7Li_1 phases. Cu(Li) are colored red (green). (For interpretation of the references to color in this figure legend, the reader is referred to the Web version of this article.)

space group $Fd\bar{3}m$. Interestingly, Li atoms simply form a diamond lattice in this structure, while Cu atoms form many tetrahedron units embedded in the lithium framework. All the lengths of Cu-Cu bonds in the tetrahedron unit are 2.454 Å, which are also shorter than those in fcc Cu. It's important to note that there are some Cu-Li intermetallics with high copper content such as Cu_5Li_1, Cu_6Li_1, Cu_7Li_1, Cu_8Li_1, and so on. Among these high copper content compounds, Cu_7Li_1 is a thermodynamically stable phase, while the other phases are slightly above the convex hull and might exist as metastable phases. The stable Cu_7Li_1 has a triclinic structure with space group $P\bar{1}$, the Cu atoms in which also form tetrahedron units or planar triangle units, while lithium atoms are embedded in the mixed two kinds of the units. The lattice parameters of the other metastable stoichiometric alloys are also listed in Table S2. Although these compounds have comparatively higher formation enthalpies, they can provide some references for the investigations on the physical properties of Cu-Li intermetallic compounds as a function of Cu concentration. In fact, both Cu_4Li and Cu_2Li_3 were believed to exist in the previous work [6–11]. We noticed that Cu_2Li_3 has been reported experimentally by Peng et al. [38] to be a metastable phase. The latest experimental research by Li et al. [12] also did not support the existence of stable Cu_2Li_3 and Cu_4Li phases. In this paper, we searched the structures for Cu_4Li and Cu_2Li_3 up to 25 atoms in a unit cell. However, we found that Cu_4Li and Cu_2Li_3 phases are not thermodynamically stable at atmospheric pressure, in agreement with the works [12,38]. In fact, we want to point out that the minimum formation enthalpy of Cu-Li alloys is about −0.069 eV/atom, which is much higher than that of Au-Li alloys (−0.653 eV/atom). The comparatively high formation enthalpy may be the reason that the previous experimental work cannot synthesize the ordered Cu-Li alloys easily. Thus we suggest that the Cu-Li intermetallic compounds might be synthesized using some special approaches such as application of hydrostatic pressure and application of low temperature.

3.2. Electronic structures and dynamical stability

To get a better understanding of the chemical bonding properties of *Fmmm* Cu_1Li_2, $Fd\bar{3}m$ Cu_2Li_1 *and* $P\bar{1}$ Cu_7Li_1, the band structures, total density of states (TDOS) and partial density of states (PDOS) of the three structures were calculated, which are shown in Fig. 3(a), (b) and (c),respectively. In Fig. 3, the dashed red lines all correspond to the Fermi level, which was assigned at 0 eV.

As can be seen from Fig. 3, for all three phases, there are band overlaps between the valence band and the conduction, indicating that they all exhibit normal metallic behaviors. Furthermore, Cu-3d states of the three phases are the highest in the composition of valence states and mostly responsible for bond formations. For *Fmmm* Cu_1Li_2, besides Cu-3d states, Li-2*p* and Cu-4*p* states also make considerable contributions near the Fermi level, while Li-2s states only show very small contribution. For $Fd\bar{3}m$ Cu_2Li_1 *and* $P\bar{1}$ Cu_7Li_1, the states of copper are more dominant than those of lithium, and Cu-3d and Cu-*4p* states show prominent contributions at the Fermi level.

In order to reflect their bonding nature directly, we further investigated the electron density difference of three stable Cu-Li compounds, which is defined as: $\Delta\rho = \rho_{sc} - \rho_{atom}$, where ρ_{sc} is the total charge density obtained after self-consistent calculations, and ρ_{atom} is the total charge density obtained after non-self-consistent calculations. Although three stable phases are metallic, the covalent bonds can be found in these structures. For *Fmmm* Cu_1Li_2 as shown in Fig. 4(a), the co-planar Cu atoms form covalent bonds, and lithium atoms between the Cu-layers also possess some degrees of covalent character. For $Fd\bar{3}m$ Cu_2Li_1 in Fig. 4(b), the distances between the lithium atoms are relatively large, thus they cannot form covalent bonds effectively. However, the Cu-Cu bonds still remain covalent nature, the electron transformations are mainly concentrated around tetrahedron units. $P\bar{1}$ Cu_7Li_1 are similar with Cu_1Li_2 and Cu_2Li_1, the covalent character is also found among Cu-Cu bonds.

To further investigate the characteristics of chemical bonding in the stable Cu-Li phases, we also performed the Mulliken atomic population and Mulliken overlap population (MOP) calculations, which are shown in Table S3 and Table S4, respectively. Mulliken bond population calculation is a very useful tool for evaluating the bonding character in a material. It is acknowledged that a positive

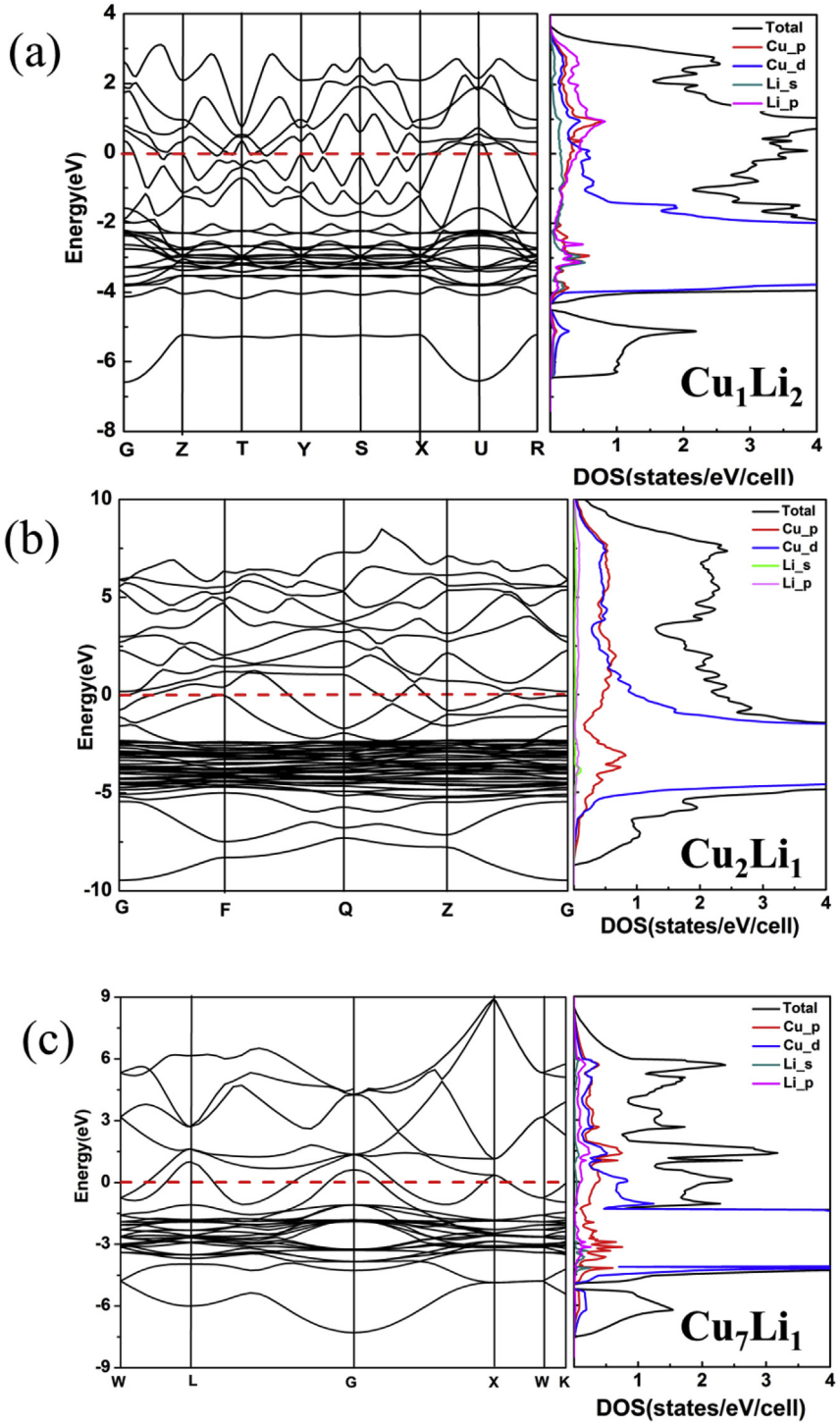

Fig. 3. The band structures and densities of states of (a) Cu_1Li_2, (b) Cu_2Li_1 and (c) Cu_7Li_1 at the ground state.

value of the bond population indicates a covalent bond, and a negative value indicates an anti-bonding state, while a zero value implies a perfect ionic bond. For all three phases, the charge transfers from Li to Cu are observed as seen from Table S3, which indicate the ionic character in the internal of Cu-Li. Furthermore, all the Mulliken bond populations of the Cu-Li bonds have negative values as shown in Table S4, which also reveal the ionic character between Cu and Li atoms originated from the electronegativity difference. However, the Mulliken bond populations of Cu-Cu bonds are positive, so covalent bonds are found between copper atoms, in agreement with the analysis of the electron density difference maps.

Although *Fmmm* Cu_1Li_2, $Fd\bar{3}m$ Cu_2Li_1 and $P\bar{1}$ Cu_7Li_1 phases are thermodynamically stable at ambient condition, one phase that can exist stably must be dynamically stable. Therefore, we calculated the phonon dispersion curves, total and partial phonon density of states of *Fmmm* Cu_1Li_2, $Fd\bar{3}m$ Cu_2Li_1 and $P\bar{1}$ Cu_7Li_1, which are

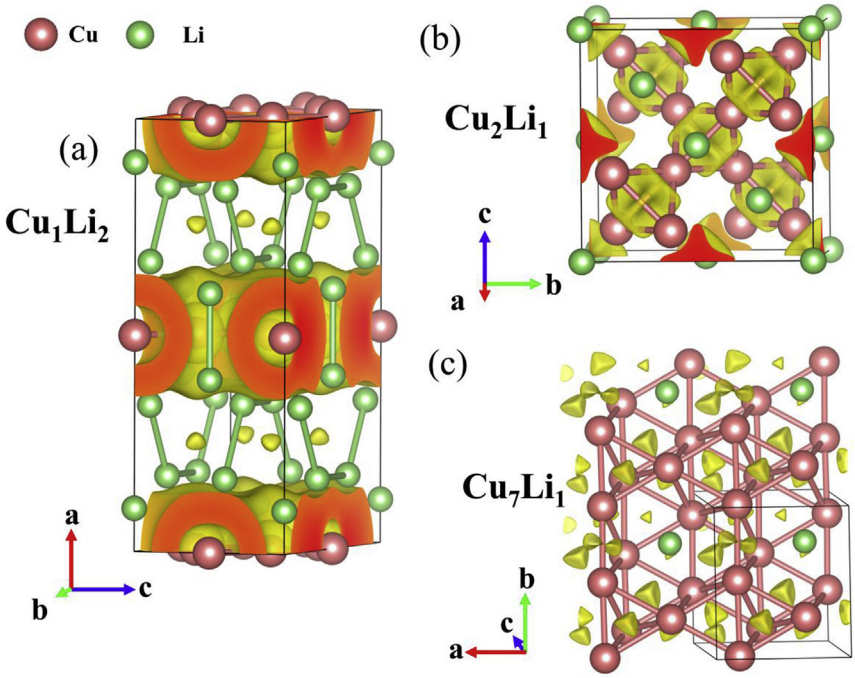

Fig. 4. The three-dimensional charge density difference map for (a) Cu_1Li_2, (b) Cu_2Li_1 and (c) Cu_7Li_1 at ground state. Cu(Li) are colored red (green). (For interpretation of the references to color in this figure legend, the reader is referred to the Web version of this article.)

displayed in Fig. S1(a), (b) and (c), respectively. In Fig. S1, the absence of any imaginary phonon frequencies in the entire Brillouin zone tells us that all the three phases are dynamically stable at 0 GPa and 0 K.

3.3. Elastic and thermodynamical properties

The elastic constants can provide much valuable information of a material directly or indirectly, which involves many different properties such as structure stability, brittleness, ductility, hardness, anisotropy and propagation of elastic waves. Hence, the study of elastic constants is very meaningful for a full-scale investigation of the mechanical properties of Cu-Li alloys. We calculated the elastic constants using a stress-strain method [39]. All the calculated elastic constants of Cu-Li compounds are shown in Table S5. We first investigated the mechanical stabilities of all the newly found structures. The mechanical stability of intermetallic compounds requires that strain energy must be positive, which requires that all the principal minor determinants of the elastic constant matrix C_{ij} should be all positive, the detail formulas can be found in Ref [40]. With the help of this criterion, by simple calculations, we revealed that Cu–Li compounds mentioned above are all mechanically stable at the ground state.

We further calculated the bulk modulus (B), shear modulus (G), and Young's modulus (E) from the elastic constants. Theoretically, bulk modulus (B) is a measure of resistance to volume change, shear modulus (G) is a measure of resistance to reversible deformations upon shear stress [41,42], while Young's modulus (E) is often used to describe the stiffness property in intermetallic compounds. The larger the values of B and G, the stronger are the abilities of resisting to the volume and shear deformations, respectively, while the larger value of E, the stiffer is the material [41,43,44]. We calculated the bulk modulus (B) and shear modulus (G) by using the Voigte-Reusse-Hill method [45], respectively. The specific formulas for all the structures can be expressed as following:

$$B = 0.5*(B_V + B_R) \quad (2)$$

$$G = 0.5*(G_V + G_R) \quad (3)$$

where the subscript V represents the Voigt bounds [46], and R denotes the Reuss bounds [47]. The values of B_V,B_R,G_V and G_R in Cu-Li compounds can be obtained using elastic stiffness constants C_{ij} and elastic compliance coefficients S_{ij} [48,49]. The Young's modulus (E) was computed using the relationship [45]:

$$E = 9BG/(3B + G) \quad (4)$$

Fig. 5 shows the three moduli as a function of copper content.

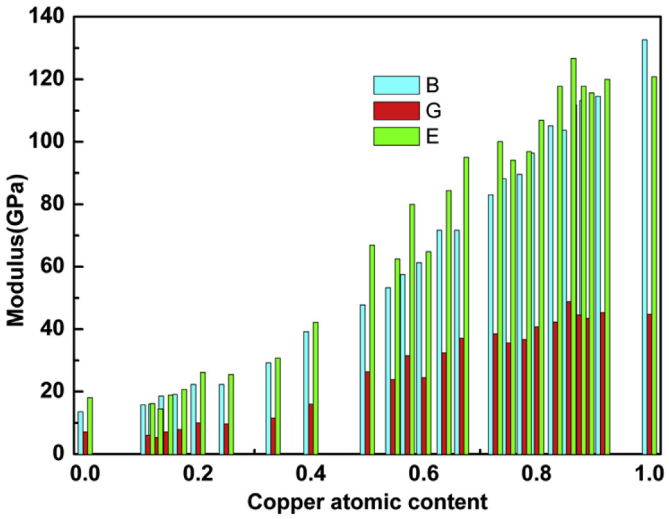

Fig. 5. The calculated bulk modulus (B), shear modulus (G) and Young's modulus (E) as a function of Cu concentration.

For the Cu-Li alloys, the bulk modulus B, shear modulus G and Young's modulus E are in the range of 13.6–132.6 GPa, 5.4–48.8 GPa and 14.5–126.7 GPa, respectively. Since we have predicted so many binary Cu-Li intermetallic compounds, we can get approximate relationships between the elastic moduli and the copper content. The data of the three moduli (B, G and E) verse Cu content were fitted, respectively. The obtained fitting formulas are listed as following:

$$y_B = 12.1 + 25.3x + 97.9x^2 \quad (5)$$

$$y_G = 7.4 - 26.6x + 168.1x^2 - 102.9x^3 \quad (6)$$

$$y_E = 19.3 - 66.6*x + 422.9*x^2 - 251.1*x^3 \quad (7)$$

where x, y_B, y_G and y_E are the copper content, bulk modulus, shear modulus and Young's modulus of Cu-Li intermetallic compounds, respectively. As Cu content increases, the Young's modulus E increases most rapidly, then the bulk modulus B, and finally the shear modulus G. According to the previous electronic structure analysis, copper atoms tend to form covalent bonds, and the increasing Cu content results in more covalent bonds formed in the Cu-Li intermetallic compounds. Theoretically, more covalent bonds formed in a crystal are favorable for the increase of the elastic modulus, so it is natural that the three elastic moduli increase with Cu-content increasing.

Poisson's ratio is another fundament physical quantity of the ordered alloy, which is defined as the ratio of transverse strain to axial strain [50]. The Poisson's ratio ν can be computed using the relationship [45]:

$$\nu = (3B - 2G)/(6B + 2G) \quad (8)$$

Theoretically, Poisson's ratio is bound between −1 and 0.5 for isotropic elastic materials. The bigger Poisson's ratio generally means the better plasticity [51]. To confirm the brittle and ductile properties of Cu-Li alloys, we also calculated the ratio of shear modulus to bulk modulus [41]. The reference value is 0.57, which is used to separate brittle and ductile nature [43]. If G/B < 0.57, the material is ductile and vice versa. In addition, the lower the G/B ratio, the better the ductility [52,53]. Fig. 6 shows that the Poisson's ratios for Cu-Li system are in the range of 0.25 and 0.35, so all the predicted Cu-Li compounds behave in a ductile manner. Notably, the Poisson's ratios for *Fmmm* Cu_1Li_2, $Fd\bar{3}m$ Cu_2Li_1, and $P\bar{1}$ Cu_7Li_1 are 0.324, 0.303, and 0.324, respectively. From Fig. 6, we can see that none of the G/B values of Cu-Li compounds is higher than 0.57, in agreement with the results of Poisson's ratio. Thus we can conclude that all the Cu-Li compounds are ductile materials.

We further estimated the hardness of the Cu-Li compounds using a simple relation [54]:

$$H_V = 0.1475G \quad (9)$$

Fig. 7 shows the relationship between copper content and Vickers hardness H_v in Cu-Li compounds. It is found that the hardness values of the Cu-Li alloys are in the range of 0.8–7.2 GPa, which are very small on the whole. The overall trend for H_v is to increase with increasing Cu content. According to equation (9), the hardness values of *Fmmm* Cu_1Li_2, $Fd\bar{3}m$ Cu_2Li_1 and $P\bar{1}$ Cu_7Li_1 are found to be 1.7, 5.5, and 6.6 GPa, respectively. Similar with the elastic moduli, the increase of copper content leads to more covalent bonds formed in the Cu-Li intermetallic compounds, which may be responsible for the increase of H_v with copper content.

Elastic anisotropy of crystalline materials plays a critical role in various applications including phase transformations [55], anisotropic plastic deformation [56], crack behavior [57], and so on. Many different ways are widely used to characterize the anisotropy of crystal materials, for instance, the universal anisotropic index (A^U), the compression and shear percent anisotropies (A_B and A_G). A^U, A_B, and A_G can be determined via the moduli [58,59]. $A^U = 0$ represents locally isotropic materials, while $A^U > 0$ denotes the extent of material anisotropy. Furthermore, the larger the value of A^U is, the higher the degree of elastic anisotropy in the material is. For A_B and A_G, a value of zero represents elastic isotropy, and a value of one is the largest anisotropy.

The following equations have been used to calculate A^U, A_B, and A_G.

$$A^U = 5G_V/G_R + B_V/B_R - 6 \quad (10)$$

$$A_B = (B_V - B_R)/(B_V + B_R) \times 100\% \quad (11)$$

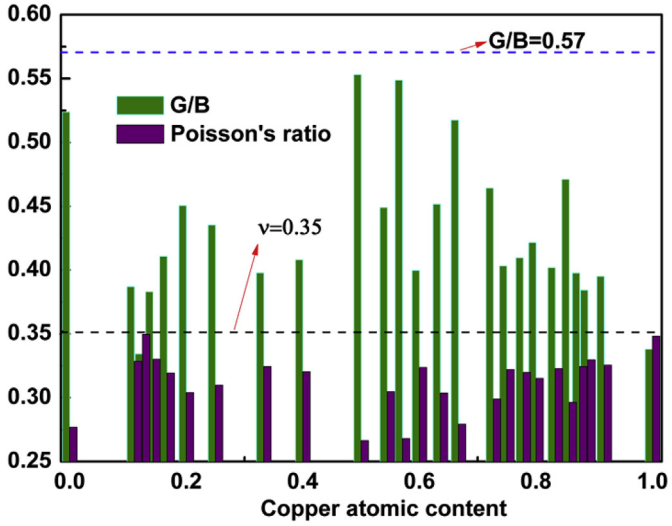

Fig. 6. Calculated G/B and Poisson's ratio ν of Cu–Li compounds as a function of Cu concentration.

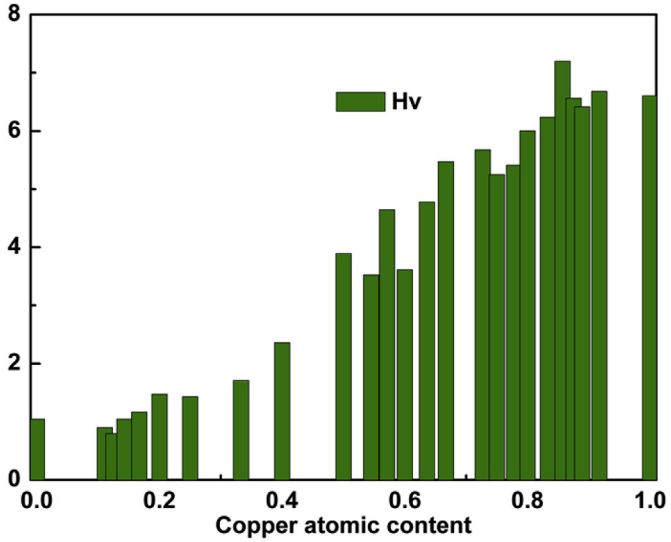

Fig. 7. Calculated hardness H_V of Cu–Li compounds as a function of Cu concentration.

$$A_G = (G_V - G_R)/(G_V + G_R) \times 100\% \quad (12)$$

Fig. 8 shows that A^U, A_B and A_G change with Cu content. It is found that A^U>0 for all Cu-Li compounds, therefore all the Cu-Li alloys exhibit anisotropic elasticity to a certain extent. The A^U values of *Fmmm* Cu_1Li_2, $Fd\bar{3}m$ Cu_2Li_1, and $P\bar{1}$ Cu_7Li_1 are 1.91, 0.02 and 1.69, respectively, thus both *Fmmm* Cu_1Li_2 and $P\bar{1}$ Cu_7Li_1 exhibit a larger anisotropy, while $Fd\bar{3}m$ Cu_2Li_1 shows nearly elastic isotropy. We noticed that the percentage elastic anisotropy in compression (A_B) is smaller than that in shear (A_G) for each of the predicted Cu-Li compounds. The A_B and A_G values of *Fmmm* Cu_1Li_2 are 0.06 and 0.16, respectively, while those of $P\bar{1}$ Cu_7Li_1 are 0.0 and 0.15, respectively. Evidently, the shear moduli for *Fmmm* Cu_1Li_2 and $P\bar{1}Cu_7Li_1$ are both anisotropic, and the bulk modulus of *Fmmm* Cu_1Li_2 shows weaker anisotropy, while the bulk modulus of $P\bar{1}$ Cu_7Li_1 is isotropic. For cubic phase $Fd\bar{3}m$ Cu_2Li_1, both the calculated A_B and A_G are closed to 0, indicating that bulk modulus and shear modulus of Cu_2Li_1 are nearly isotropic.

The Debye temperature $\mathbf{\Theta_D}$ is an appropriate parameter to describe some phenomena of solid-state physics, which are associated with specific heat, the stability of lattices and melting points. Moreover, the $\mathbf{\Theta_D}$ is often used to estimate the strength of covalent bonds in solids. It, therefore, makes sense to calculate the $\mathbf{\Theta_D}$ values of Cu-Li compounds. On the other hand, as far as we know, there is temporarily no experimental data of the $\mathbf{\Theta_D}$ of Cu-Li compounds. The calculation results may provide some references for the experimental study of Cu-Li compounds in the future. We took one semi-empirical formula to calculate the Debye temperature which is closely related to the average sound velocity. The formula adopted is given in detail as follows [60]:

$$\Theta_D = (h/k)[(3n/4\pi)(N_A\rho/M)]^{1/3}\nu_m \quad (13)$$

where h, k, and n are the Planck's constant, Boltzmann's constant, and the number of atoms per formula unit, respectively. N_A, ρ and M are the Avogadro constant, density and molecular weight, respectively.

The average sound velocity ν_m can be obtained from the longitudinal and shear sound velocities (ν_l and ν_s) via the following equation:

$$\nu_m = \left[(1/3)\left(2/\nu_s^3 + 1/\nu_l^3\right)\right]^{-1/3} \quad (14)$$

where ν_l is closely related to the elastic moduli and density, and ν_s is determined by shear modulus G and density ρ.The formulas related to the ν_l and ν_s are as follows [61]:

$$\nu_l = [(3B + 4G)/3\rho]^{1/2} \quad (15)$$

$$\nu_s = (G/\rho)^{1/2} \quad (16)$$

Table 1 shows the values of ν_m, ν_l, ν_s and Debye temperatures at 0 K and 0 GPa. On the whole, the velocities of Cu-Li compounds increase oscillatorily with Cu-content increasing, so do Debye temperatures. The Debye temperatures of Cu-Li compounds vary in the range from 259.9 K to 366.7 K. Generally, the larger the Debye temperature is, the stronger the covalent bonds are [62]. As we have mentioned, Cu atoms trend to form the covalent bonds in the Cu-Li alloys, so the increasing Cu content will lead to more covalent bonds formed, and hence the strength of covalent bonds increases with Cu content on the whole. The change of Debye temperature with Cu content just proves above empirical law. For the three stable compounds, As shown in Table 1, the Debye temperature of $Fd\bar{3}m$ Cu_2Li_1 is slightly higher than Debye temperatures of *Fmmm* Cu_1Li_2 and $P\bar{1}$ Cu_7Li_1. This means that the covalent bonds in Cu_2Li_1 compound are slightly stronger than those in Cu_1Li_2 and Cu_7Li_1. Concerning Debye temperature, there is also another rule of thumb, a greater Debye temperature generally means a larger associated thermal conductivity [63]. Thus as the most stable phase, Cu_2Li_1 should possess the best thermal conductivity relative to the other two stable Cu–Li compounds.

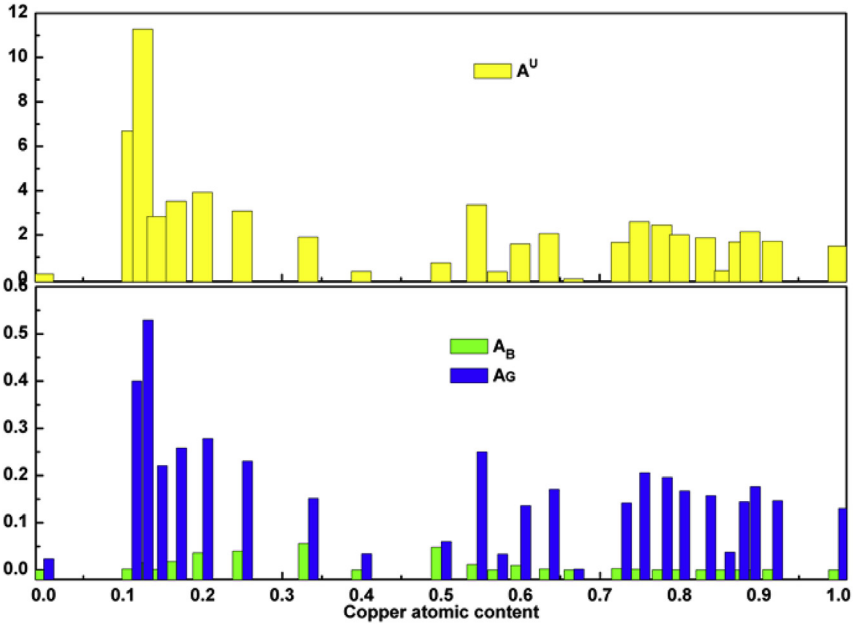

Fig. 8. Calculated universal anisotropic index (A^U), compression and shear percent anisotropies (A_B and A_G) of Cu–Li compounds as a function of Cu concentration.

Table 1
Density ρ (g/cm^3), shear sound velocity v_s (m/s), longitudinal sound velocity v_l (m/s), average sound velocity v_m (m/s) and Debye temperature Θ_D (K) of Cu_xLi_y binary alloys at 0 K and 0 GPa.

	Crystal system	ρ	v_s	v_l	v_m	Θ_D
Cu_1Li_8	triclinic	1.195	2259	4472	2533	285.7
Cu_1Li_7	triclinic	1.290	2037	4237	2291	259.9
Cu_1Li_6	triclinic	1.440	2223	4416	2493	286.8
Cu_1Li_5	orthorhombic	1.475	2307	4479	2583	291.1
Cu_1Li_4	triclinic	1.689	2439	4597	2725	309.8
Cu_1Li_3	triclinic	2.222	2092	3985	2339	277.7
Cu_1Li_2	orthorhombic	2.663	2089	4097	2341	275.9
Cu_2Li_3	cubic	3.383	2173	4227	2434	296.9
Cu_1Li_1	hexagonal	4.051	2554	4526	2840	347.1
Cu_6Li_5	triclinic	4.848	2222	4194	2484	314.8
Cu_4Li_3	hexagonal	5.089	2489	4422	2770	352.2
Cu_6Li_4	triclinic	4.941	2226	4360	2494	309.9
Cu_7Li_4	triclinic	5.654	2393	4506	2674	341.8
Cu_2Li_1	cubic	5.325	2640	4771	2941	363.8
Cu_8Li_3	triclinic	6.467	2441	4559	2726	351.0
Cu_2Li_1	triclinic	6.709	2303	4497	2580	333.3
Cu_7Li_2	triclinic	6.929	2301	4471	2577	333.1
Cu_4Li_1	triclinic	7.125	2389	4598	2674	345.9
Cu_5Li_1	monoclinic	7.427	2385	4663	2672	346.4
Cu_6Li_1	hexagonal	7.606	2534	4711	2829	366.7
Cu_7Li_1	triclinic	7.774	2391	4691	2680	347.8
Cu_8Li_1	triclinic	7.876	2350	4663	2635	341.9
$Cu_{11}Li_1$	monoclinic	8.104	2364	4647	2649	343.9

4. Conclusion

In this paper, to resolve a longstanding controversy concerning the existence of the Cu-Li intermediate phases, we have investigated the stability of Cu-Li intermetallic compounds using the first-principles calculations coupled with the variable-composition evolutionary algorithm in USPEX. The correlations between Cu concentration and the overall performances of Cu-Li compounds have been studied systematically. The main research results are summarized as follows:

(1) We revealed that the formation enthalpy is negative for the Cu-Li intermetallic compounds at zero temperature and zero pressure, indicating the Cu-Li intermediate compounds can be synthesized at ambient condition. Three Cu-Li intermediate compounds, *Fmmm* Cu_1Li_2, $Fd\bar{3}m$ Cu_2Li_1 and $P\bar{1}$ Cu_7Li_1, are found to be stable in the view of thermodynamics, dynamics and mechanics.
(2) Although the three stable alloys exhibit the metallic character, covalent bonds between copper atoms and ionic bonds between lithium-copper atoms are found in these compounds. Furthermore, 3d states of copper atoms play an important role in the Cu-Li alloy and are mostly responsible for bond formations.
(3) The bulk modulus B, shear modulus G, Young's modulus E, Vicker hardness H_v of the Cu-Li alloys are in the range of 13.6–132.6 GPa, 5.4–48.8 GPa, 14.5–126.7 GPa and 0.8–7.2 GPa, respectively. More importantly, B, G, E and H_v of Cu-Li compounds are found to be related to Cu concentration. Cu atoms are found to trend to form the covalent bonds in the Cu-Li alloys, the increasing Cu content leads to more covalent bonds formed. So with an increase of copper content, the three elastic moduli, Vicker hardness and Debye temperature increase on the whole. In addition, the fitting formulas which describe the approximate relationships between Cu content and elastic moduli are given in detail.
(4) The Poisson's ratios for Cu-Li system are in the range of 0.25–0.35, and most Cu-Li compounds are found to have good ductility.
(5) The percentage elastic anisotropy in compression (A_B) is smaller than that in shear (A_G) for all the predicted Cu-Li compounds.
(6) The velocities and Debye temperatures increase with Cu-content increasing as a whole. The Debye temperatures of Cu-Li compounds vary in the range from 259.9 K to 366.7 K. As the most stable phase, $Fd\bar{3}m$ Cu_2Li_1 has the highest Debye temperature relative to the other stable Cu–Li compounds.

The current investigations provide essential information for the Cu–Li intermetallic compounds, which will stimulate the future experiments on the structural, mechanical and thermodynamic properties measurements.

Acknowledgement

This work is supported in China by the National Natural Science Foundation of China (Grant Nos. 51501093, 41773057, 11364009, U1304612, and U1404608), Science Technology Innovation Talents in Universities of Henan Province (No.16HASTIT047), Young Core Instructor Foundation of Henan Province (No. 2015GGJS-122). The structural figures in this paper were plotted using VESTA software.

Appendix A. Supplementary data

Supplementary data related to this article can be found at https://doi.org/10.1016/j.jallcom.2018.07.020.

References

[1] D.C. Zhu, M.Z. Song, J.Z. Chen, M.J. Tu, H.B. Pan, Electrical conductivity of Cu-Li alloys, J. Cent. South Univ. Technol. 11 (2004) 252–254.
[2] S. Pastorello, Thermal analysis of the system lithium-copper, Gazz. Chim. Ital. 60 (1930) 988–992.
[3] W. Klemm, B. Volavšek, Zur kenntnis des systems lithium–kupfer, Z. Anorg. Allg. Chem. 296 (1958) 184–187.
[4] A.D. Pelton, The Cu– Li (Copper-Lithium) system, J. Phase Equilib. 7 (1986) 142–144.
[5] N. Saunders, System Cu–Li, in: I. Ansara, A.T. Dinsdale, M.H. Rand (Eds.), COST 507 Thermochemical Database for Light Metal Alloys, vol. 2, 1998, pp. 168–169. Luxembourg.
[6] C.F. Old, P. Trevena, Reaction in copper-lithium system and its implications for liquid-metal embrittlement, Met. Sci. 15 (1981) 281–286.
[7] A. Penaloza, M. Ortiz, C.H. Worner, An electrodeposition method to obtain Cu-Li alloys, J. Mater. Sci. Lett. 14 (1995) 511–513.
[8] H.U. Borgstedt, C. Guminski, Cu-li, International Union of Pure and Applied Chemistry, Oxford, 1996, p. 59.
[9] A. Van de Walle, Z. Moser, W. Gasior, First-principles calculation of the Cu-Li phase diagram, Arch. Metall. Mater. 49 (2004) 535–544.
[10] W. Gąsior, B. Onderka, Z. Moser, A. Dębski, T. Gancarz, Thermodynamic evaluation of Cu–Li phase diagram from EMF measurements and DTA study, Calphad 33 (2009) 215–220.
[11] H. Okamoto, Cu-Li (Copper-Lithium), J. Phase Equilib. Diff. 32 (2011), 172-172.
[12] D. Li, S. Fürtauer, H. Flandorfer, D.M. Cupid, Thermodynamic assessment of the Cu–Li system and prediction of enthalpy of mixing of Cu–Li–Sn liquid alloys, Calphad 53 (2016) 105–115.
[13] X.W. Zhang, G. Trimarchi, A. Zunger, Possible pitfalls in theoretical determination of ground-state crystal structures: the case of platinum nitride, Phys. Rev. B 79 (2009), 092102.
[14] G.C. Yang, Y. Wang, F. Peng, A. Bergara, Y. Ma, Gold as a 6p-element in dense lithium aurides, J. Am. Chem. Soc. 138 (2016) 4046–4052.
[15] C.Y. Pu, D.W. Zhou, Y.L. Song, Z. Wang, F.W. Zhang, Z.W. Lu, Phase transition and thermodynamic properties of YAg alloy from first-principles calculations, Comput. Mater. Sci. 102 (2015) 21–26.
[16] Z.W. Lu, D.W. Zhou, P.J. Bai, C. Lu, Z.G. Zhong, G.Q. Li, Theoretical investigation on structural and thermodynamic properties of the inter-metallic compound in Mg–Zn–Ag alloy under high pressure and high temperature, J. Alloys. Compd. 550 (2013) 406–411.
[17] D.W. Zhou, T.C. Su, H.Z. Song, C. Lu, Z.G. Zhong, Z.W. Lu, C.Y. Pu, Ab-initio study of phase stability, elastic and thermodynamic properties of AlY alloy under pressure, J. Alloys. Compd. 648 (2015) 67–74.
[18] C.Y. Pu, X.C. Xun, H.Z. Song, F.W. Zhang, Z.W. Lu, D.W. Zhou, Prediction of pressure-induced structural transition and mechanical properties of MgY from first-principles calculations, Commun. Theor. Phys. 65 (2016) 92–98.
[19] C.W. Glass, A.R. Oganov, N. Hansen, USPEX—evolutionary crystal structure prediction, Comput. Phys. Commun. 175 (2006) 713–720.

[20] A.R. Oganov, C.W. Glass, Crystal structure prediction using ab initio evolutionary techniques: principles and applications, J. Chem. Phys. 124 (2006), 244704.
[21] Y.M. Ma, A.R. Oganov, Y. Xie, High-pressure structures of lithium, potassium, and rubidium predicted by an ab initio evolutionary algorithm, Phys. Rev. B 78 (2008), 014102.
[22] A.R. Oganov, J. Chen, C. Gatti, Y.Z. Ma, Y.M. Ma, C.W. Glass, Z.X. Liu, T. Yu, O.O. Kurakevych, V.L. Solozhenko, Ionic high-pressure form of elemental boron, Nature 457 (2009) 863.
[23] D.F. Duan, X.L. Hunag, D. Li, H.Y. Yu, Y.X. Liu, Y.B. Ma, B.B. Liu, T. Cui, Pressure-induced decomposition of solid hydrogen sulfide, Phys. Rev. B 91 (2015), 180502.
[24] D.F. Duan, Y.X. Liu, F.B. Tian, D. Li, X.L. Hunag, Z.L. Zhao, H.Y. Yu, B.B. Liu, W.J. Tian, T. Cui, Pressure-induced metallization of dense $(H_2S)_2H_2$ with high-T_c superconductivity, Sci. Rep. 4 (2014) 6968.
[25] A. BILIĆ, J.D. Gale, M.A. Gibson, N. Wilson, K. McGregor, Prediction of novel alloy phases of Al with Sc or Ta, Sci. Rep. 5 (2015) 9909.
[26] Y.B. Ma, D.F. Duan, Z.J. Shao, H.Y. Yu, H.Y. Liu, F.B. Tian, X.L. Huang, D. Li, B.B. Liu, T. Cui, Divergent synthesis routes and supercon- ductivity of ternary hydride $MgSiH_6$ at high pressure, Phys. Rev. B 96 (2017), 144518.
[27] A. Bouibes, A. Zaoui, High-pressure polymorphs of $ZnCO_3$:Evoluti- onary crystal structure prediction, Sci. Rep. 4 (2014) 5172.
[28] G. Kresse, J. Hafner, Ab initio molecular dynamics for liquid metals, Phys. Rev. B 47 (1993) 558.
[29] G. Kresse, J. Furthmüller, Efficiency of ab-initio total energy calcul- ations for metals and semiconductors using a plane-wave basis set, Comput. Mater. Sci. 6 (1996) 15–50.
[30] P.E. Blöchl, O. Jepsen, O.K. Andersen, Improved tetrahedron method for Brillouin-zone integrations, Phys. Rev. B 49 (1994) 16223.
[31] J.P. Perdew, K. Burke, M. Ernzerhof, Generalized gradient approximation made simple, Phys. Rev. Lett. 77 (1996) 3865.
[32] M.D. Segall, P.J. Lindan, M.A. Probert, C.J. Pickard, P.J. Hasnip, S.J. Clark, M.C. Payne, First-principles simulation: ideas, illustrations and the castep code, J. Phys. Condens. Matter 14 (2002) 2717.
[33] D. Vanderbilt, Soft self-consistent pseudopotentials in a generalized eigenvalue formalism, Phys. Rev. B 41 (1990) 7892.
[34] K. Parlinski, Z.Q. Li, Y. Kawazoe, First-principles determination of the soft mode in cubic ZrO_2, Phys. Rev. Lett. 78 (1997) 4063.
[35] A. Togo, F. Oba, I. Tanaka, First-principles calculations of the ferroelastic transition between rutile-type and $CaCl_2$-type SiO_2 at high pressures, Phys. Rev. B 78 (2008), 134106.
[36] K. Momma, F. Izumi, VESTA 3 for three-dimensional visualization of crystal, volumetric and morphology data, J. Appl. Crystallogr. 44 (2011) 1272–1276.
[37] E.Y. Tonkov, E.G. Ponyatovsky, Phase Transformations of Elements under High Pressure, CRC Press, Boca Raton, FL, 2005.
[38] L.Z. Peng, J. Wu, F. Ding, S.X. Zhao, L. Qiao, H.M. Mao, P. Wang, G.N. Luo, Effect of Li on safety of Cu components for EAST, J. Fusion Energy 34 (2015) 1009–1015.
[39] R. Yu, J. Zhu, H.Q. Ye, Calculations of single-crystal elastic constants made simple, Comput. Phys. Commun. 181 (2010) 671–675.
[40] F. Milstein, Theoretical strength of a perfect crystal, Phys. Rev. B 3 (1971) 1130.
[41] S.F. Pugh, XCII. Relations between the elastic moduli and the plastic properties of polycrystalline pure metals, Philos. Mag. A 45 (1954) 823–843.
[42] A.F. Young, C. Sanloup, E. Gregoryanz, S. Scandolo, R.J. Hemley, H.K. Mao, Synthesis of novel transition metal nitrides IrN_2 and OsN_2, Phys. Rev. Lett. 96 (2006), 155501.
[43] P. Mao, B. Yu, Z. Liu, F. Wang, Y. Ju, First-principles calculations of structural, elastic and electronic properties of AB_2 type intermetallics in Mg–Zn–Ca–Cu alloy, J. Magn. Alloys 1 (2013) 256–262.
[44] X. Yang, A. Hao, X. Wang, X. Liu, Y. Zhu, First-principles study of structural stabilities, electronic and elastic properties of BaF_2 under high pressure, Comput. Mater. Sci. 49 (2010) 530–534.
[45] R. Hill, Elastic properties of reinforced solids: some theoretical principles, J. Mech. Phys. Solid. 11 (1963) 357–372.
[46] W. Voigt, A Determination of the Elastic Constants for Beta-Quartz. Lehrbuch de Kristallphysik(Terubner,Leipzig), Springer, California, 1928.
[47] A. Reuss, Calculation of the flow limits of mixed crystals on the basis of the plasticity of monocrystals, Z. Angew. Math. Mech. 9 (1929) 49–58.
[48] Z.J. Wu, E.J. Zhao, H.P. Xiang, X.F. Hao, X.J. Liu, J. Meng, Crystal structures and elastic properties of superhard IrN_2 and IrN_3 from first principles, Phys. Rev. B 76 (2007), 054115.
[49] D.Y. Liu, X.F. Dai, X.H. Wen, G.W. Qin, X.Y. Meng, Predictions on the compositions, structures, and mechanical properties of intermediate phases in binary Mg–X (X= Sn, Y, Sc, Ag) alloys, Comput. Mater. Sci. 106 (2015) 180–187.
[50] Q.Y. Fan, Q. Wei, C.C. Chai, H.Y. Yan, M.G. Zhang, Z.Z. Lin, Z.X. Zhang, J.Q. Zhang, D.Y. Zhang, Structural, mechanical, and electronic properties of P3m1-BCN, J. Phys. Chem. Solid. 79 (2015) 89–96.
[51] Y. Cao, J.C. Zhu, Y. Liu, Z.S. Nong, Z.H. Lai, First-principles studies of the structural, elastic, electronic and thermal properties of Ni_3Si, Comput. Mater. Sci. 69 (2013) 40–45.
[52] M.M. Zhong, X.Y. Kuang, Z.H. Wang, P. Shao, L.P. Ding, X.F. Hua- ng, Phase stability, physical properties, and hardness of transition-metal diborides MB_2 (M= Tc, W, Re, and Os): first-principles investigations, J. Phys. Chem. C 117 (2013) 10643–10652.
[53] B. Wang, D.Y. Wang, Y.X. Wang, A new hard phase of ReB_4 predicted from first principles, J. Alloys Compd. 573 (2013) 20–26.
[54] X. Jiang, J.J. Zhao, X. Jiang, Correlation between hardness and elastic moduli of the covalent crystals, Comput. Mater. Sci. 50 (2011) 2287–2290.
[55] A. Schmitz, M. Chandrasekaran, G. Ghosh, L. Delaey, Elastic anisotropy and the substitutional bainite formation in copper base alloys, Acta Metall. 37 (1989) 3151–3155.
[56] C.S. Man, On the correlation of elastic and plastic anisotropy in sheet metals, J. Elast. 39 (1995) 165–173.
[57] V. Tvergaard, J.W. Hutchinson, Microcracking in ceramics induced by thermal expansion or elastic anisotropy, J. Am. Chem. Soc. 71 (1988) 157–166.
[58] Y.H. Duan, Z.Y. Wu, B. Huang, S. Chen, Phase stability and anisotropic elastic properties of the Hf–Al intermetallics: a DFT calculation, Comput. Mater. Sci. 110 (2015) 10–19.
[59] F. Li, Y.H. Man, C.M. Li, J.P. Wang, Z.Q. Chen, Mechanical properties, minimum thermal conductivity, and anisotropy in bc-structure superhard materials, Comput. Mater. Sci. 102 (2015) 327–337.
[60] L. Fu, Y.H. Zhao, L. Yang, Y.P. Duan, K. Ge, P.D. Han, Electronic and elastic properties of Al_4Ce binary compound under pressure via first-principles, Superlattice. Microst. 69 (2014) 76–86.
[61] P. Wachter, M. Filzmoser, J. Rebizant, Electronic and elastic properties of the light actinide tellurides, Physica B 293 (2001) 199–223.
[62] Q. Chen, Z.W. Huang, Z.D. Zhao, C.K. Hu, Thermal stabilities, elastic properties and electronic structures of B_2-MgRE (RE= Sc, Y, La) by first-principles calculations, Comput. Mater. Sci. 67 (2013) 196–202.
[63] P.G. Klemens, Solid State Physics: Advances in Research and Applications, vol. 7, Academic Press, New York, 1958, pp. 1–99.